A numerical study of peristaltic flow

By

MinSu Yun

Submitted for the degree of

Master of Engineering (Research)

Faculty of Engineering and Information Technology

University of Technology, Sydney (UTS)

Australia

2009

CERTIFICATE

I certify that this thesis has not already been submitted for any degree and is not being submitted as part of candidature for any other degree.

I also certify that the thesis has been written by me and that any help that I have received in preparing this thesis, and all sources used, have been acknowledged in this thesis.

Signature of Candidate

....

Acknowledgements

I would like to thank Dr Phuoc Huynh for his valuable advice and encouragement during the course of this work. Dr Huynh has provided important insights and has been flexible, patient and a valuable source of knowledge.

I also thank Phyllis Agius who helped me greatly in concentrating on this research. I want to thank her for all her support, expertise and general trouble shooting.

I would like to dedicate this work to my parents, Choi, Eunna and Yun, Yunsik for their support throughout the course of this study.

Abstract

Peristaltic flow is a transport mechanism primarily used in the human body to transport fluids. This form of transport is characterised by the contraction and relaxation of flexible tubes. Many studies have been undertaken to investigate this phenomenon. Factors such as amplitude ratio, wave number and the Reynolds number have been studied to identify their effects on peristaltic flow.

In this work, the peristaltic flow of power-law fluids under non-isothermal conditions is investigated using the Computation Fluid Dynamics (CFD) methodology. The effect of temperature on peristaltic flow will be investigated in various conditions, for example, in Newtonian fluid (a special case of power-law fluids), non-Newtonian fluid of power-law type and different values of coefficient a_1 (a_1 being exponential coefficient of the temperature dependent viscosity).

Peristaltic flow for possible industrial applications will be considered, with fluid properties thus corresponding to those of an oil and a wider range of the Reynolds numbers (1-1000) than for biological applications. Comparison of isothermal versus non-isothermal flow shall also be shown.

Flow will be studied in the reference frame which moves with the wave (the wave frame). In this reference frame, the flow becomes steady. Firstly, isothermal flow models are shown to produce comparable results with previous works from the literature, therefore proving the validity of the present computational methodology. These conditions were then applied to non-isothermal models.

After this confidence has been established, non-isothermal flow is then investigated. This in turn affects whole flow field including factors such as change of viscosity and shear stress due to temperature change.

Streamline patterns, velocity profiles and pressure drop per wavelength are presented to show the effect of temperature in peristaltic flow. Pressure drop in non-isothermal flow is shown to be significantly less than that for isothermal case. Thus, for example, in the case of isothermal Newtonian flow, pressure drop per wavelength is 6305.2 Pa with conditions of the Reynolds number Re=10, wave number $(\alpha) = 0.25$ and amplitude ratio $(\phi) = 0.5$. On the other hand, in the case of non-isothermal flow, pressure drop per wavelength becomes 2054.7 Pa with the same conditions.

Influence of temperature is then considered in flow of non-Newtonian fluids of the power-law type. Consistent flow conditions are modelled to give a reasonable comparison. It is found that Newtonian and shear-thickening fluids are influenced by temperature strongly. However, in the case for shear thinning fluid, the effect of temperature is relatively small. Thus, for example, in table 5.2 (chapter 5), pressure drop per wavelength in a case for shear thinning fluids is very similar, at 49.153 Pa and 55.892 Pa corresponding to viscosity exponential coefficient $a_1 = -0.034\,°\mathrm{C}^{-1}$ and $a_1 = 0\,°\mathrm{C}^{-1}$ respectively.

The role of coefficient a_1 in power-law fluid is clarified in this research. Different values of a_1 are used and the corresponding results presented. They show that a_1 has stronger influence on the flow at regions adjacent to walls.

Vorticity patterns are also presented to show the effect of temperature. Especially, for Newtonian fluids, temperature affects vorticity differently at the crest and trough sections.

The effect of temperature on peristatic flow in different geometry is shown by streamline patterns, pressure drops and velocity profile. The variable, h (the mean distance of the wall from the axis of symmetry) is utilised to produce a model that shows the effect of the geometry in isothermal flow. After the geometry is changed and resulting effect plotted, non-isothermal flow model is considered to prove the presence of thermal effects. The results gained by the models indicate that the temperature effect is stronger at the region adjacent to the wall in different geometries and the effect of temperature reduced the effect of geometry in pressure drop.

The above study was carried out in order to simulate realistic peristaltic flow. The addition of temperature by modelling non-isothermal flow has been shown to reduce the impact of the Reynolds number therefore changing the streamline pattern. This effect has been visualised in a number of special fluid applications to give a variety of results. The effects shown visually by CFD represent what peristaltic flow in industrial applications could look like.

TABLE OF CONTENTS

Title page	i
Certificate	ii
Acknowledgement	iii
Abstract	iv
Table of Contents	vii
Nomenclature	xii
List of Units	xiv
List of the Figures	xiv
List of the Tables	xvii
List of the Pictures	xvii

CHAPTER 1 Introduction

1.1 Introduction	1-2
1.2 Brief history of the study of peristaltic flow	1-3
1.3 Problem statement and research objectives	1-4
1.4 Thesis Outline	1-5

CHAPTER 2 LITERATURE REVIEW

2 Literature Review

2.1 Introduction	2-2
2.1.1 Peristaltic pumping	2-3
2.1.1.1) Basic mechanism of peristaltic pumping	2-3
2.1.1.2) Parameters of the problem	2-5
2.1.1.3) Trapping	2-5

2.1.2 Numerical analysis of two-dimensional peristaltic 2-6
2.1.2.1) Periodicity of the flow pattern 2-6
2.1.2.2) Effect of the geometrical shape of the peristaltic wave 2-8
2.1.2.3) The effect of the Reynolds number 2-9
2.1.3 Numerical study of two-dimensional peristaltic flow 2-9
2.1.3.1) Velocity field 2-10
2.1.3.2) Pressure field 2-12
2.1.4 A Numerical investigation of peristaltic waves in circular tubes 2-15
2.1.4.1) Flow structure, pressure, shear stress distribution for zero time mean flow 2-15
2.1.4.2) Reynolds number effect corresponding to the case when $\alpha \rangle 0.01$ 2-20
2.1.5 On mechanism of the peristaltic flow for power-law fluid 2-21
2.1.5.1) Pressure drop per wavelength with power-law fluid 2-21
2.1.5.2) The behaviour of axial velocity for three values of m 2-22
2.1.5.3) The effect of ϕ, F and m on dp/dz 2-23

2.2 Background
2.2.1 Introduction 2-25
2.2.2 Definition of peristaltic flow 2-26
2.2.3 Reynolds number 2-27
2.2.4 Definition of periodic wave 2-29
2.2.5 Governing equation 2-30
2.2.5.1) Power-law fluid 2-30
2.2.5.2) Conservation of mass 2-33
2.2.5.3) Conservation of momentum 2-34
2.2.5.4) Balance of energy 2-35
2.2.5.5) Boundary conditions-general consideration 2-34

CHAPTER 3 METHODOLOGY

3.1 Introduction 3-2

3.2 Computation Fluid Dynamics (CFD) 3-3

3.2.1 Modelling 3-4

3.2.2 CFD-ACE applications 3-6

3.2.2.1 Flow module 3-6

3.2.2.2. Heat transfer module 3-6

1) Thermal field calculation 3-6

3.2.2.3 Control panel 3-7

1) Volume Condition (VC) 3-7

2) Boundary Condition (BC) 3-9

3.2.2.4 CFD-VIEW 3-13

3.2.2.5 CFD-GEOM 3-14

3.3 Grid Convergence 3-15

CHAPTER 4 ISOTHERMAL FLOW

4.1 Introduction 4-2

4.2 The max and min axial velocity in simulation results 4-2

4.2.1 Results 4-3

4.3 The effect of the Reynolds number on the streamline pattern 4-7

4.3.1 Results 4-8

4.4 The effect of the Reynolds number on the streamline pattern for $\frac{\bar{Q}}{\pi c h^2} = 0.6$ 4-10

4.4.1 Modification of Inlet condition for the case of $\frac{\bar{Q}}{\pi c h^2} = 0.6$ 4-11

4.4.2 Result 4-15

4.5 Summary of isothermal flow 4-16

CHAPTER 5 NON-ISOTHERMAL FLOW

5.1 Introduction 5-2

5.2 The effect of temperature in Newtonian flow for the case when $\alpha = 0.25$, $\phi = 0.5$ over a wide range of the Reynolds number 5-4

5.2.1 Results 5-6

5.3 The effect of temperature on power-law fluids 5-12

5.3.1 Results 5-13

5.4 The effect of exponential coefficient a_1 of viscosity on peristaltic flow for Newtonian fluid 5-20

5.4.1 Results 5-21

5.5 Vorticity patterns and pressure contour in non-isothermal flow with Newtonian fluid and thinning fluid when Re=1 5-25

5.5.1 Results 5-26

5.6 The effect of temperature on different geometries with non-isothermal flow in Newtonian fluid 5-30

5.6.1 Results 5-32

5.7 Summary of non-isothermal flow 5-37

CHAPTER 6 CONCLUSION AND RECOMMENDATION

6.1 Conclusions 6-2

6.2 Recommendations 6-6

References R-1

Appendix A-1

Nomenclature

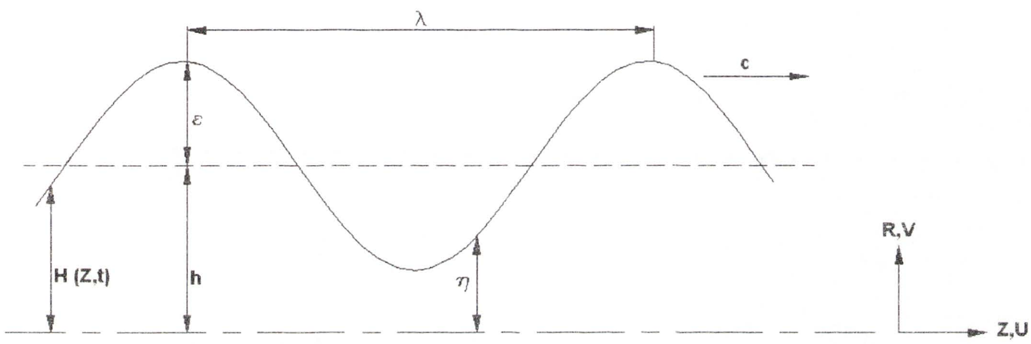

Configuration of peristaltic flow

c	=	the wave speed (m/s)
C_p	=	specific heat capacity ($J\,g^{-1}K^{-1}$)
F	=	non-dimensional volume flow rate in the wave frame ($\frac{q}{ch}$)
h	=	mean distance (m)
$\bar{\ell}$	=	the dimensionless time-average flow rate in the laboratory frame
n	=	power-law index
$\Delta \bar{p}_\lambda$	=	the dimensionless pressure rise per wavelength
q	=	the rate of fluid flow in the wave frame (m^3/s)
$\bar{Q}$	=	the time-average rate of volume flow in the laboratory frame (m^3/s)
R	=	the radial coordinate in laboratory frame (m)
r	=	the radial coordinate in wave frame (m)
Re	=	Reynolds number

T	=	temperature ($°C$)
t	=	time (sec)
U	=	the axial velocity in Laboratory frame (V_z) (m/s)
u	=	the axial velocity in wave frame (v_z) (m/s)
V	=	the radial velocity in laboratory frame (V_r) (m/s)
v	=	the radial velocity in wave frame (v_r) (m/s)
Z	=	the axial coordinate in laboratory frame (m)
z	=	the axial coordinate in wave frame (m)
α	=	wave number ($\frac{h}{\lambda}$)
$\dot{\gamma}$	=	the local calculated shear rate (s^{-1})
$\dot{\gamma}_0$	=	the cut off shear rate (s^{-1})
ε	=	the wave amplitude (m)
$\eta_{(r)}$ *or* η	=	the displacement of wall (m)
λ	=	the wavelength (m)
μ	=	dynamic fluid viscosity ($Kg/(m \cdot s)$)
μ_0	=	the zero-shear-rate viscosity ($Kg/(m \cdot s)$)
ν	=	kinematic fluid viscosity (m^2/s)
v_s	=	mean fluid velocity (m/s)
ρ	=	fluid density (kg/m^3)
ϕ	=	amplitude ratio ($\frac{\varepsilon}{h}$)

List of Units

Angle	=	deg	(degree)
Energy	=	J	(joule)
Force	=	N	(newton)
Length	=	m	(meter)
Mass	=	Kg	(kilogram)
Time	=	s	(second)
Temperature	=	$°C$	(degree Celsius)

List of Figures

Figure 2.1 Conceptual illustration of peristaltic pumping 2-3

Figure 2.2 Nomenclature for 2-dimensional periodic sine wave 2-4

Figure 2.3 Streamlines in a wave frame when a trapped bolus exists in the laboratory frame 2-5

Figure 2.4 Velocity profiles ; $\phi = 0.19$, $\alpha = 0.21$, Re=210 and $\bar{Q} = 0$ 2-7

Figure 2.5 Velocity profiles ; $\phi = 0.4$, $\alpha = 0.3$, Re=0.01 and $\bar{Q} = 0$ 2-8

Figure 2.6 Velocities on the centre axis at the crest and the trough section for $\phi = 0.2, \alpha = 0.01$ and $\bar{\ell} = 0$ 2-9

Figure 2.7 Longitudinal velocity profiles $\phi = 0.4, \alpha = 0.2$ Re=1 $\Delta p_\lambda = 0$ 2-11

Figure 2.8 Velocities on the centre axis at the crest and the trough section for Re=0.01 2-12

Figure 2.9 Pressure distribution along peristaltic wall for ϕ =0.4, α =0.2 and Δp_λ =0 2-13

Figure 2.10 Pressure rise per wave number for Re=0.01, $\bar{\ell} = 0$ 2-14

Figure 2.11 The effect of the Reynolds number on the streamline patterns

	in the wave frame and laboratory frame for α =0.01, $\bar{Q}/\pi ch = 0$ and $\phi = 0.2$	2-16
Figure 2.12	The effect of the Reynolds number on the streamline patterns in the wave frame and laboratory frame for $\alpha = 0.01$ $\bar{Q}/\pi ch = 0$ and $\phi = 0.7$	2-17
Figure 2.13	The effect of the Reynolds number on the normalized pressure distribution for $\alpha = 0.01$ and $\bar{Q}/\pi ch = 0$,(a) $\phi = 0.2$ (b) $\phi = 0.7$	2-18
Figure 2.14	The effect of the Reynolds number on the shear stress distribution for $\alpha = 0.01$ and $\bar{Q}/\pi ch = 0$,(a) $\phi = 0.2$ (b) $\phi = 0.7$	2-19
Figure 2.15	The effect of the Reynolds number on the maximum axial velocity for different wave number α (a) $\phi = 0.2$ (b) $\phi = 0.4$	2-20
Figure 2.16	Radial distribution of the axial velocity for a position with dimensionless tube radius of h=1 for three different values of m when F=-1 (a) and F=-2 (b)	2-22
Figure 2.17	Distribution of the pressure gradient dp/dz within a wavelength $z \in [0,2\pi]$ for F=-1 and ϕ=0.2 (a), F=-2 and ϕ=0.2 (b) and F=-1 and ϕ=0.4 (c)	2-23
Figure 2.18	Movement of fluid by contraction and relaxation sequence	2-26
Figure 2.19	An example of periodic waves	2-29
Figure 2.20	Rectangle and cylindrical coordinate for equations below	2-33
Figure 2.21	Configuration of peristaltic flow in two-dimensional axi-symmetric Tube	2-36
Figure 3.1	Computational model of the peristaltic flow	3-4
Figure 3.2	Dimension for the geometry (unit: m): $\alpha = 0.25$, $\phi = 0.5$	3-5
Figure 3.3	Example of structured face and an activated volume condition	3-8
Figure 3.4	Input for density (a),specific heat capacity (b) and thermal conductivity (c)	3-8
Figure 3.5	Inputs for viscosity properties	3-9
Figure 3.6	Illustration of BC type and BC settings inputs	3-10
Figure 3.7	Boundary value regions	3-10

Figure 3.8	Input for the parametric input panel	3-11
Figure 3.9	Inputs for (a) Inlet, (b) Outlet, (c) Wall and (d) Symmetry	3-13
Figure 3.10	Window of CFD-VIEW	3-14
Figure 3.11	Grid points and meshes in a CFD model	3-15
Figure 3.12	Arrangement of points to measure pressure change and velocity	3-16
Figure 3.13	Comparison of pressure drop (Pa) per wavelength with the number of grids applied in a wave cycle (For Newtonian and isothermal flow)	3-17
Figure 3.14	Comparison of velocity (m/s) with the number of grids applied in a wave cycle (for Newtonian and isothermal flow)	3-18
Figure 3.15	Comparison of pressure drop (Pa) per wavelength with the number of grids applied in a wave cycle (For Newtonian and non-isothermal flow)	3-19
Figure 3.16	Comparison of velocity (m/s) with the number of grids applied in a wave cycle (for Newtonian and non-isothermal flow)	3-20
Figure 3.17	Temperature change per wave cycle in non-isothermal flow	3-23
Figure 3.18	Dimension for Geometry; $\alpha = 0.25$, $\phi = 0.5$	3-24
Figure 4.1	The comparison of the max and min axial velocity in simulation result with $\alpha = 0.01$, the Reynolds number=0.01	4-3
Figure 4.2	The effect of the Reynolds number on the (U/c)max of the U velocity for α=0.01, zero flow rate and different values of amplitude ratio	4-5
Figure 4.3	The comparison of the effect of the Reynolds number on the streamline patterns in the wave frame for $\alpha = 0.01$, zero flow rate and $\phi = 0.7$	4-8
Figure 4.4	The flow rate q and u profile	4-12
Figure 4.5	The effect of the Reynolds number on the streamline patterns in the wave frame for $\alpha = 0.01$, $\phi = 0.7$, $\bar{Q}/\pi c h^2 = 0.6$	4-15
Figure 5.1	Arrangement of measurement points	5-5
Figure 5.2	Variation of Pressure drop when isothermal flow ($a_1 = 0\ 1/{}^{\circ}C$) and non-isothermal flow ($a_1 = -0.034\ 1/{}^{\circ}C$) in a wide range of the Reynolds	

number 5-7

Figure 5.3 Velocity profile on the crest section in a_1=0 (left) and a_1=-0.034 °C^{-1} (right) 5-8

Figure 5.4 Velocity profile on the trough section in a_1=0 (left) and a_1=-0.034 °C^{-1} (right) 5-9

Figure 5.5 Comparison of the streamline patterns with different value of $\bar{Q}/\pi h^2 c$ for the case when $a_1 = 0$ °C^{-1} (left) and $a_1 = -0.034$ °C^{-1} (right) in Re=10 5-10

Figure 5.6 Comparison of the variation of streamline in shear thinning fluid (in the wave frame) for the case when a_1=0 (left) and a_1=-0.034 (right) 5-13

Figure 5.7 Comparison of the variation of streamline in Newtonian fluid (in the wave frame) for the case when a_1=0 (left) and a_1=-0.034 °C^{-1} (right) 5-15

Figure 5.8 Comparison of the variation of streamline in shear thickening fluid (in the wave frame) for the case when a_1=0 (left) and a_1=-0.034 °C^{-1} (right) 5-17

Figure 5.9 Change in Pressure drop (Pa) along Power-law index when Re=1 (ΔP Over Wavelength: λ=0.02m) 5-20

Figure 5.10 Comparison of streamline in different values of coefficient a_1=0, a_1=-0.02 and a_1=-0.04 °C^{-1} 5-22

Figure 5.11 The variation of velocity profile in the crest section with different values of coefficient a_1 when Re=1 5-23

Figure 5.12 The variation of velocity profile in the trough section with different values of coefficient a_1 when Re=1 5-24

Figure 5.13 Comparison of the variation of vorticity in non-isothermal flow and isothermal flow with Newtoninan fluid when Re=1 5-27

Figure 5.14 Comparison of the variation of vorticity for shear thinning fluid 5-28

Figure 5.15 The comparison of vorticity profile between isothermal and non-isothermal flow in the crest section with Newtonian fluid when Re=1 (r : radial direction) 5-28

Figure 5.16 The comparison of vorticity profile between isothermal and non-isothermal flow in the trough section with the condition of Newtonian fluid when Re=1 (r : radial direction) 5-29

Figure 5.17 Pressure contour for the condition of isothermal and non-isothermal Flow 5-30

Figure 5.18 Configuration of peristaltic flow in two-dimensional axi-symmetric Tube 5-31

Figure 5.19 Comparison of the variation of streamline in different geometry (in the wave frame) for the case when $a_1 = 0$ °C^{-1} (left) and $a_1 = -0.034$ °C^{-1} (right) 5-33

Figure 5.20 Change in pressure drop per wavelength in the three different geometries with the case of isothermal and non-isothermal flow when n=1 (Newtonian fluid) 5-34

Figure 5.21 Comparison of velocity profile in the three geometries with the case of isothermal flow in the crest section (Newtonian fluid) 5-35

Figure 5.22 Comparison of velocity profile in the three geometries with the case of non-isothermal flow in the crest section (Newtonian fluid) 5-36

Figure 5.23 Comparison of velocity profile in the three geometries with the case of isothermal flow (left) and non-isothermal flow (right) in the trough section (Newtonian fluid) 5-37

List of Tables

Table 2.1 Pressure drop per wavelength along flow direction ΔP_λ for different values of total flux F, the wave amplitude ϕ and non-Newtonian parameter m. 2-21

Table 2.2 Axial velocities at the center of the cylindrical tube listed for various values of m and total flux F 2-22

Table 3.1 Comparison of changes in axial velocity and pressure drop with different numbers of order convergence 3-3

Table 4.1 Comparison of Xiao's results and the present work for α =0.01 verse ϕ =0.2, 0.4 and 0.6 with Reynolds number = 0.01 and $\bar{\ell} = 0$ 4-4

Table 4.2 Comparison of Xiao's results and the present work for α =0.01 verse ϕ =0.2, 0.4 and 0.6 with Reynolds number = 0.1 and $\bar{\ell} = 0$ 4-6

Table 5.1 Pressure drop (ΔP) and Temperature change (ΔT) per wavelength along the flow direction with Newtonian fluid 5-6

Table 5.2 Comparison of Pressure drop (Δp) and Temperature change (ΔT) along flow direction in Newtonian and Non-Newtonian fluid for the case of Re=1 5-19

Table 5.3 Comparison of Pressure drop(ΔP) in a wavelength between $a_1 = -0.02$ °C^{-1} and $a_1 = -0.04$ °C^{-1} with Newtonian fluid for the case of Re=1 5-25